Since January 2020 Elsevier has created a COVID-19 resource centre with free information in English and Mandarin on the novel coronavirus COVID-19. The COVID-19 resource centre is hosted on Elsevier Connect, the company's public news and information website.

Virology 433 (2012) 440–448

Contents lists available at SciVerse ScienceDirect

Virology

journal homepage: www.elsevier.com/locate/yviro

Identification and characterization of RNA duplex unwinding and ATPase activities of an alphatetravirus superfamily 1 helicase

Qinrong Wang, Yajuan Han, Yang Qiu, Shaoqiong Zhang, Fenfen Tang, Yan Wang, Jiamin Zhang, Yuanyang Hu *, Xi Zhou *

State Key Laboratory of Virology, College of Life Sciences, Wuhan University, Wuhan, Hubei 430072, China

ARTICLE INFO

Article history:
Received 4 July 2012
Returned to author for revisions
24 August 2012
Accepted 28 August 2012
Available online 17 September 2012

Keywords:
Dendrolimus punctatus tetravirus
Protein Hel
Helicase
NTPase
RNA duplex unwinding

ABSTRACT

Dendrolimus punctatus tetravirus (DpTV) belongs to the genus omegatetravirus of the *Alphatetraviridae* family. Sequence analysis predicts that DpTV replicase contains a putative helicase domain (Hel). However, the helicase activity in alphatetraviruses has never been formally determined. In this study, we determined that DpTV Hel is a functional RNA helicase belonging to superfamily-1 helicase with 5′–3′ dsRNA unwinding directionality. Further characterization determined the length requirement of the 5′ single-stranded tail on the RNA template and the optimal reaction conditions for the unwinding activity of DpTV Hel. Moreover, DpTV Hel also contains NTPase activity. The ATPase activity of DpTV Hel could be significantly stimulated by dsRNA, and dsRNA could partially rescue the ATPase activity abolishment caused by mutations. Our study is the first to identify an alphatetravirus RNA helicase and further characterize its dsRNA unwinding and NTPase activities in detail and should foster our understanding of DpTV and other alphatetraviruses.

Introduction

The *Alphatetraviridae* is a family of positive-stranded (+) RNA viruses, which are the family of viruses with nonenveloped icosahedral $T=4$ viral particles, and also the family of RNA viruses that restrictively infect insects, particularly the *Lepidoptera* (Hanzlik and Gordon, 1997; Speir and Johnson, 2008). Previously, tetraviruses, whose capsids share a common $T=4$ symmetry, had been classified as a single family called *Tetraviridae*. Recently, this group of viruses has been re-classified into three families, i.e., *Alphatetraviridae*, *Carmotetraviridae* and *Permutotetraviridae* (http://www.ictvonline.org/virusTaxonomy.asp?version=2011), based on their genome organizations and translation products (Adams and Carstens, 2012; Dorrington, 2011; Walter et al., 2010; Zeddam et al., 2010). For the *Alphatetraviridae* family, two genera are classified, including betatetravirus and omegatetravirus. Betatetraviruses, such as *Nudaurelia capensis* β virus (NβV), have a single genomic RNA of ~6.5 kilobase (kb) and a pitted particle surface, while omegatetraviruses, such as *N. capensis* ω virus (NωV) and *Helicoverpa armigera* stunt virus (HaSV), have bipartite genomic RNAs (RNA1: ~5.3 kb; RNA2: ~2.5 kb) and particle surface with oval protrusions (Olson et al., 1990; Speir and Johnson, 2008; Speir et al., 2010; Taylor et al., 2006).

Tetraviruses in all the three families have attracted a lot of attentions due to their close evolutionary linkage with nodaviruses, another family of (+)RNA viruses, such as Flock House virus (FHV) and Wuhan nodavirus (WhNV), that have $T=3$ capsids and are well recognized as models for studying viral RNA replication, antiviral innate immunity and nonenveloped virus entry into cells (Odegard et al., 2010; Qi et al., 2011, 2012; Qiu et al., 2011; Speir et al., 2010; Walukiewicz et al., 2006). The capsids of both tetraviruses and nodaviruses undergo autoproteolytic maturation processing and yield small γ peptides that are lipophilic and may function to disrupt host membranes for viral entry (Bothner et al., 2005; Speir et al., 2010; Tang et al., 2009; Taylor et al., 2002; Tomasicchio et al., 2007; Walukiewicz et al., 2006). Moreover, previous structural studies uncovered numerous structural similarities between tetraviruses and nodaviruses, suggesting that the capsids of tetraviruses are evolutionarily derived from those of nodaviruses, and carmotetravirus is evolutionarily more primordial and closer to nodaviruses than omegatetravirus (Johnson et al., 1994; Speir et al., 2010). Interestingly, omegatetraviruses have a bipartite genome, like nodaviruses, while the genome of carmotetravirus is monopartite (Cai et al., 2010; Speir and Johnson, 2008). On the other hand, the replicases of omegatetraviruses belong to alpha-like viral replicase (Ahlquist et al., 1985; Koonin et al., 1992; Sabanadzovic et al., 2009; Yi et al., 2005; Zeddam et al., 2010), making the evolution of tetraviruses, particularly omegatetraviruses, more complicated and interesting. Therefore, a better understanding of the biology of omegatetraviruses may provide novel insights into conserved or unconserved biological characteristics of the *Alphatetraviridae* family.

Dendrolimus punctatus tetravirus (DpTV) was isolated from diseased *D. punctatus* (pine moth) from Yunnan Province, China and has been identified as an omegatetravirus (Dorrington, 2011; Yi et al., 2005; Zhou et al., 2006). Although the International

* Corresponding authors.
E-mail addresses: zhouxi@whu.edu.cn (X. Zhou), yyhu@whu.edu.cn (Y. Hu).

0042-6822/$ - see front matter © 2012 Elsevier Inc. All rights reserved.
http://dx.doi.org/10.1016/j.virol.2012.08.045

Committee on Taxonomy of Viruses renamed it as *D. punctatus* virus (DpV) in 2009 (http://www.ictvonline.org/virusTaxonomy.asp?version=2009), in this study we still use the name of DpTV to avoid possible confusion, as the abbreviation of *Dasychira pudibunda* virus, a betatetravirus, is also DpV. Our group studies both nodavirus (Qi et al., 2011, 2012; Qiu et al., 2011) and alphatetravirus (Yi et al., 2005; Zhou et al., 2006, 2008), and therefore, we decided to embark on a systematic characterization of the molecular biology of alphatetravirus, particularly DpTV. Here, we reported such an effort aimed to characterize the putative helicase of alphatetravirus.

Helicases normally utilize the energy generated from nucleoside triphosphate (NTP) hydrolysis to translocate along and unwind the helical structure of dsDNA or dsRNA (Mackintosh and Raney, 2006; Singleton et al., 2007). Helicases are classified into six superfamilies (SF), SF-1 to SF-6 (Gorbalenya and Koonin, 1993; Gorbalenya et al., 1989; Karpe and Lole, 2010; Singleton et al., 2007). Among them, SF-1 and SF-2 are the two largest and most closely related superfamilies, which are generally monomers containing at least seven conserved motifs (I, Ia, II, III, IV, V, and VI) that mediate DNA/RNA-binding, NTP binding, NTP hydrolysis or conformational change of helicases (Caruthers and McKay, 2002; Fairman-Williams et al., 2010; Gorbalenya et al., 1988; Hodgman, 1988). To date, many (+)RNA viruses are found to encode their own helicases, and helicases are found to be essential for RNA replication of numerous (+)RNA viruses, such as brome mosaic virus (BMV) (Ahola et al., 2000; Wang et al., 2005), poliovirus (Mirzayan and Wimmer, 1992; Teterina et al., 1992), flavivirus (Gu et al., 2000), alphavirus (Rikkonen, 1996) and nidovirus (van Dinten et al., 2000).

For alphatetraviruses, they encode a large viral RNA replicase protein (DpTV: ~180 kDa, HaSV: ~187 kDa, NβV: ~215 kDa). On the basis of the amino acid sequences, some alphatetraviral replicases, including NβV and all omegatetraviruses, were predicted to contain three putative domains indicative of methyltransferase (MT), RNA helicase (Hel), and RNA-dependent RNA polymerase (RdRp) (Gordon et al., 1995, 1999; Hanzlik and Gordon, 1997; Pringle et al., 1999; Short et al., 2010; Yi et al., 2005; Zeddam et al., 2010). Despite the importance of helicases in (+)RNA viruses, helicase activity in alphatetraviruses has not been formally determined, and consequently, the molecular mechanisms of helicase-mediated unwinding of alphatetraviral dsRNA have not yet been studied, which hinders our understanding of this family of viruses.

Here, we demonstrate that DpTV Hel is a functional RNA helicase with 5′–3′ unwinding directionality, and further characterized this first alphatetraviral RNA helicase in detail. Our study not only represents a crucial step toward understanding the mechanism of alphatetravirus dsRNA unwinding, but also shed light on the future study of RNA helicases and dsRNA unwinding of other alphatetraviruses.

Results

DpTV Hel is a functional RNA helicase

For (+)RNA viruses, helicase plays an indispensable role in RNA replication, transcription, and protein translation as its unwinding the secondary structure of dsRNA to be recognized by related proteins (Abdelhaleem, 2010; Lohman and Bjornson, 1996; Pyle, 2008; Speir and Johnson, 2008). To investigate whether DpTV as well as other alphatetraviruses such as HaSV and NβV, encode a helicase, we compared the amino acid sequence of DpTV replicase protein with various viral RNA helicases. As shown in Fig. 1A, the putative helicase domain of DpTV (amino acids 596–835) contains all the seven conserved motifs of SF-1 helicase, of which motifs I, II, and VI have been well studied previously in other

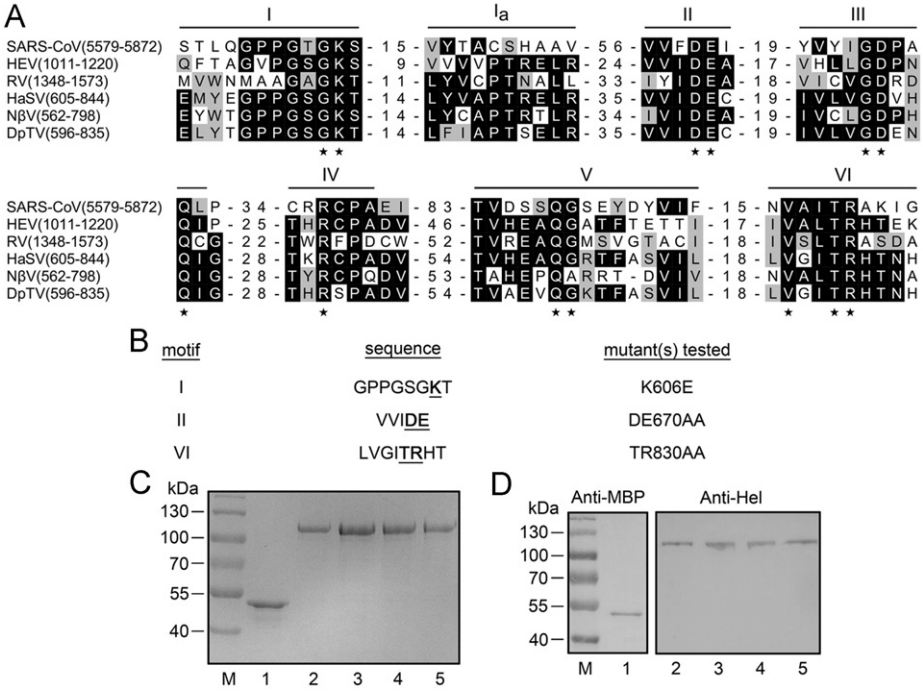

Fig. 1. (A) Amino acid sequence alignment of helicases from SARS coronavirus (SARS-CoV; GenBank: NC_004718), hepatitis E virus (HEV; GenBank: JX121233), Rubella virus (RV; GenBank: JN635296), HaSV (GenBank: NC_001981), NβV (GenBank: AF102884) and DpTV (GenBank: AY594352). Helicase motifs are labeled as motifs I to VI. (B) The mutagenesis strategy to generate point mutations in motifs I, II and VI. (C) Electrophoresis analysis of purified MBP-Hel and its mutants. Proteins were subjected to 12% SDS-PAGE, and protein bands were stained with Coomassie blue. Lane M, molecular weight markers; lane 1, MBP alone; lane 2, MBP-Hel; lane 3, MBP-Hel (I); lane 4, MBP-Hel (II); lane 5, MBP-Hel (VI). (I), (II) or (VI) indicates the mutation in motifs I, II or VI, respectively. (D) MBP-Hel and its mutants were subjected to Western blots with anti-MBP or anti-Hel polyclonal antibodies. The lanes are labeled as in (C).

helicases and demonstrated to be important for their activities. This sequence comparison suggests that this putative domain is an RNA helicase.

Our previous study showed that the putative DpTV helicase domain (Hel) did not have activity when being bacterially expressed (data not shown), indicating the necessity to use a eukaryotic system to express this protein. To determine if DpTV Hel contains the classic helicase activity, i.e., unwinding double-stranded oligonucleotides, we expressed DpTV Hel as N-terminal maltose-binding protein (MBP) fusion protein (MBP-Hel) in Baculovirus Expression System, following by protein purification (Fig. 1C and D, lane 2). Moreover, we also generated a serial of point mutations in the predicted motifs I, II and VI of DpTV Hel as indicated in Fig. 1B to investigate the potential effects of these conserved motifs on DpTV Hel unwinding activity.

To examine the unwinding activity of DpTV Hel, a short hexachloro fluorescein (HEX)-labeled RNA (RNA1) and a long non-labeled RNA (RNA3) were annealed to generate a standard dsRNA substrate with both 3′ and 5′ single-stranded tails (15 bases) (see the "Materials and methods" section). The standard substrate was incubated with DpTV Hel in unwinding reaction mixture, followed by gel electrophoresis analysis. As shown in Fig. 2A, HEX-labeled RNA strand was released from the RNA duplex substrate in the presence of DpTV Hel, $MgCl_2$ and ATP (Fig. 2A, lane 6). In addition, removing $MgCl_2$ or ATP, both of which are indispensable for most helicases activities (Huang and Liu, 2002; Shen et al., 1998; Warrener and Collett, 1995), resulted in the complete loss of unwinding activity of DpTV Hel (Fig. 2A, lanes 4 and 5). MBP alone (Fig. 2A, lane 3) or the absence of DpTV Hel (Fig. 2A, lane 1) could not support dsRNA unwinding. These results indicate that DpTV Hel is a functional RNA helicase.

We further examined whether DpTV Hel is able to unwind substrates containing DNA. To this end, we constructed three different substrates, D*/R via annealing a short HEX-labeled DNA (DNA1) and a long non-labeled RNA (RNA3), R*/D via annealing a short HEX-labeled RNA (RNA1) and a long non-labeled DNA (DNA2), and D*/D via annealing a short HEX-labeled DNA (DNA1) and a long non-labeled DNA (DNA2) (see the "Materials and methods" section). Each substrate was incubated with DpTV Hel at the same conditions as described in Fig. 2A. As shown in Fig. 2B – D, DpTV Hel could only unwind the substrate with RNA tails (D*/R) but not the substrates with DNA tails (R*/D, D*/D). These results show that DpTV Hel merely recognizes RNA template strands to unwind oligonucleotides from them, and DpTV Hel is an RNA but not a DNA specific helicase.

Furthermore, we examined the importance of the conserved SF-1 motifs on DpTV Hel dsRNA unwinding activity. To this end, the standard dsRNA substrate is incubated with MBP fusion Hel (I), Hel (II) or Hel (VI) mutant at the same conditions as described in Fig. 2A. Our results revealed that the mutations in motifs I, II, and VI dramatically reduced the dsRNA unwinding activity (Fig. 2E), thereby showing that these conserved motifs are required for DpTV Hel unwinding activity and DpTV Hel is a SF-1 RNA helicase.

Altogether, our findings from this set of experiments demonstrate that DpTV Hel is a functional RNA helicase, which belongs to SF-1 helicase superfamily.

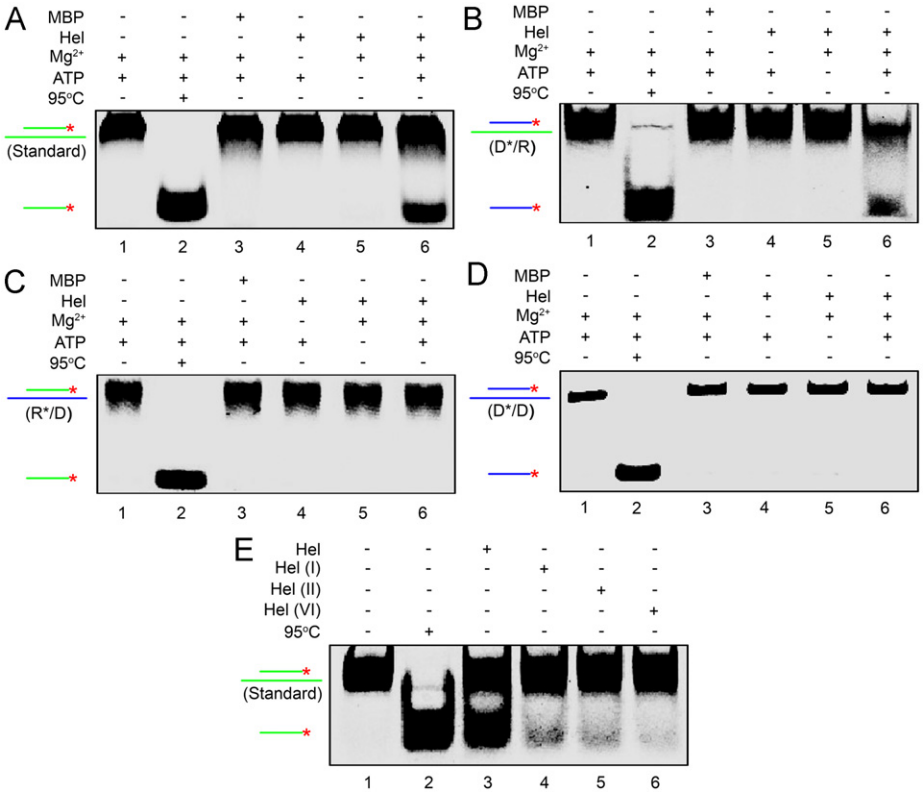

Fig. 2. Duplex unwinding activities of DpTV Hel and its mutants. (A–D) Purified MBP-Hel was incubated with standard dsRNA, dsDNA or RNA/DNA hybrid substrates in the presence or absence of Mg^{2+} or ATP (RNA: green line; DNA: blue line; HEX: red asterisk). The preparations of unwinding substrates are presented in the "Materials and methods" section. Substrates were incubated in standard reaction mixtures (except as noted) and the unwinding activity was assessed by gel electrophoresis followed by scan with a Typhoon9200. (A) Standard dsRNA substrates. (B) D*/R substrates. (C) R*/D substrates. (D) D*/D substrates. Lanes 1 and 2: reaction mixtures lacking enzyme that were either left native (lane 1) or boiled (lane 2); Lane 3, complete reaction mixture with negative control MBP alone; lanes 4 and 5, complete reaction mixtures with $MgCl_2$ omitted (lane 4) or with ATP omitted (lane 5); lane 6, complete reaction mixture. (E) dsRNA unwinding activities of DpTV Hel mutants. Lanes 1 and 2: reaction mixtures lacking enzyme that were either left native (lane 1) or boiled (lane 2); lanes 3, 4, 5 and 6, complete reaction mixture with MBP-Hel (lane 3), MBP-Hel (I) (lane 4), MBP-Hel (II) (lane 5) or MBP-Hel (VI) (lane 6). (For interpretation of the references to color in this figure legend, the reader is referred to the web version of this article.)

DpTV Hel directs the 5′–3′ dsRNA unwinding, whose efficiency is dependent on the length of the 5′ single-stranded tail on template strand

After determining that DpTV Hel is a functional helicase, we sought to examine the directionality of its RNA unwinding. To this end, several dsRNA substrates containing a 5′ single-stranded tail (15 bases), a 3′ single-stranded tail (15 bases), and blunt ends were constructed, and then reacted with MBP-Hel. As shown in Fig. 3A-C, only the dsRNA with 5′ single-stranded tail could be unwound by MBP-Hel, while 3′-tailed or blunt ended dsRNA substrates could not be unwound. These results show that DpTV Hel unwinds dsRNA in the 5′–3′ direction.

Furthermore, we examined the impact of the length of 5′ single-stranded tail on DpTV Hel unwinding activity. As illustrated in Fig. 3D, a series of dsRNA substrates with progressively decreasing lengths of 5′ single-stranded tail were generated and then reacted with MBP-Hel. The unwinding efficiency of DpTV Hel on these substrates was graphed as the percentage of the released RNA from the total dsRNA substrate at each time point. As shown in Fig. 3E, as the length of 5′ single-stranded tail decreased, the unwinding efficiency was also gradually reduced. At 60 min, the substrate release was about 44% in the presence of 15 bases single-stranded tail. When the length of 5′ single-stranded tail was reduced to three bases, only 13% RNA could be released from the dsRNA substrate. Taken together, these results indicate that DpTV Hel directs the dsRNA unwinding in the 5′–3′ direction, and its unwinding efficiency is dependent on the length of the 5′ single-stranded tail on template strand.

Optimal reaction conditions for DpTV Hel dsRNA unwinding activity

To further characterize the biochemical properties of DpTV Hel, we examined its dsRNA unwinding activity under varying reaction conditions, such as divalent metal ions, salt content and pH. The unwinding efficiency of DpTV Hel was graphed as the percentage of the released RNA from the total dsRNA substrate at each indicated reaction condition.

For helicases, Mg^{2+} is usually required for their activities (Warrener and Collett, 1995; Yang et al., 2006), and we found that DpTV Hel unwinding activity also requires the presence of Mg^{2+} (Fig. 2A). Here, we first examined whether other divalent metal ions could also support DpTV Hel function instead of Mg^{2+}. Our results showed that besides Mg^{2+}, only Mn^{2+} was able to efficiently support the unwinding activity (Fig. 4A, lanes 5 and 6). Then, we further determined the impacts of the Mn^{2+} and Mg^{2+} concentrations on DpTV Hel unwinding activity. The highest unwinding activity was observed at 2 mM $MgCl_2$ (Fig. 4B) or 4 mM $MnCl_2$ (Fig. 4C), but Mg^{2+} was preferred over Mn^{2+} under all conditions.

We further examined the effects of salt content and pH on DpTV Hel unwinding activity. The dsRNA unwinding assays with different concentrations of KCl showed that the optimal KCl concentration was around 50 mM and this helicase is relatively sensitive to KCl, as the increase of KCl from 50 mM strongly inhibited the unwinding activity of DpTV Hel (Fig. 4D). Then, under 2 mM $MgCl_2$ and 50 mM KCl, the optimal pH for the unwinding reaction was determined to a range from 7.5 to 9.0 (Fig. 4E). Taken together, we have determined the optimal reaction conditions for DpTV Hel dsRNA unwinding activity, and reaction mixture containing 2 mM $MgCl_2$ and 50 mM KCl and

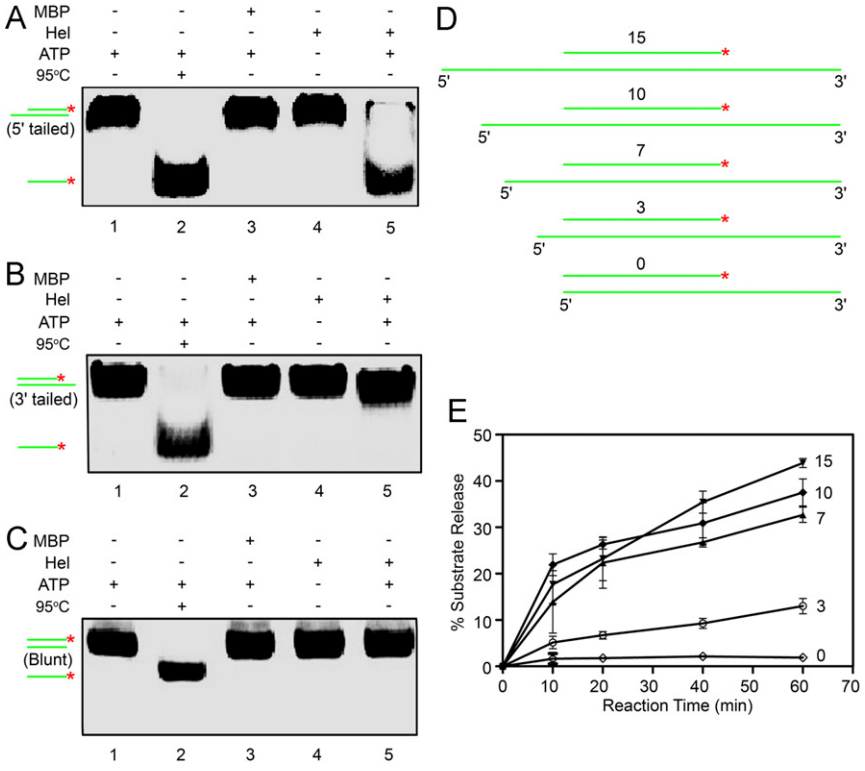

Fig. 3. DpTV Hel unwinds dsRNA in the 5′–3′ direction, and its unwinding efficiency depends on the length of 5′ single stranded tail. (A–C) MBP-Hel was reacted with 5′-tailed (A), 3′-tailed (B) or blunt ended (C) dsRNA substrates in the presence or absence of ATP. The short RNA strand was also HEX-labeled as in Fig. 2. Substrates alone (lane 1), boiled substrates (lane 2) and MBP alone (lane 3) were used as controls. (D) Schematic of the unwinding substrates with different 5′-tail length. The length of 5′ tail was indicated above each dsRNA substrate. (E) Each substrate in (D) was incubated with MBP-Hel in standard reaction condition, and the unwinding activity was graphed as the percentage of the released RNA from the total dsRNA substrate at each time point. The 5′ tail length was indicated on the right. Error bars represent S.D. values from three separate experiments.

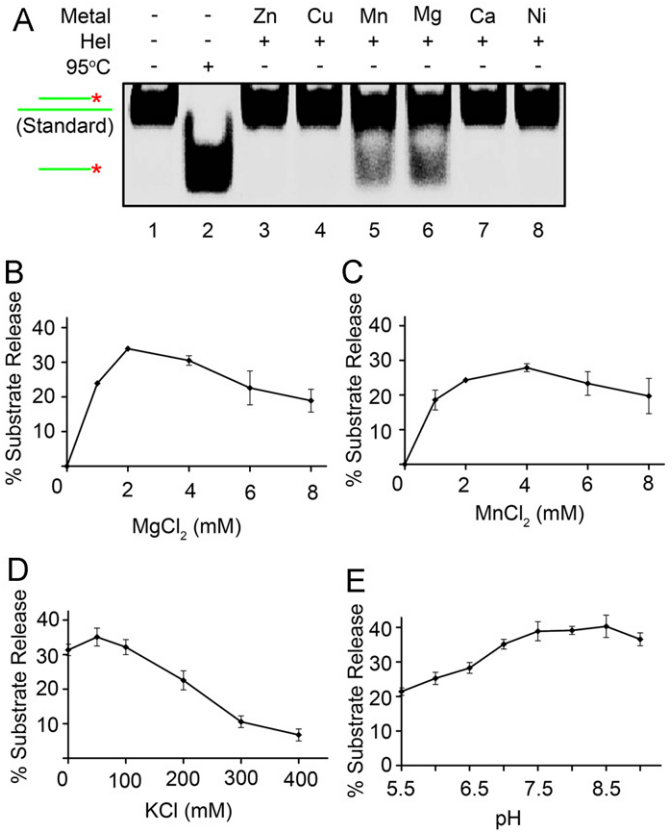

Fig. 4. Optimal conditions for DpTV Hel dsRNA unwinding. (A) Standard dsRNA substrate was reacted with MBP-Hel in the presence of 2.5 mM indicated divalent metal ions. Substrates alone or boil substrates were used as controls. (B–D) Standard dsRNA substrate was reacted with MBP-Hel in the presence of indicated concentrations of $MgCl_2$ (B), $MnCl_2$ (C) or KCl (D). The unwinding activities were determined and graphed as in Fig. 3E. (E) In the presence of 2 mM $MgCl_2$ and 50 mM KCl, the unwinding activities were determined at indicated pH, and then graphed as above. 5 mM ATP was used in all experiment, and error bars represent S.D. values from three separate experiments.

adjusted to pH 7.5 by 20 mM HEPES-KOH was used for subsequent experiments.

DpTV Hel contains the NTPase activity

To drive dsRNA unwinding, helicases usually require NTP hydrolysis to provide energy. We previously showed that the dsRNA unwinding activity of DpTV Hel depended on the presence of ATP (Fig. 2A). Thus, we sought to examine whether DpTV Hel also contains the NTPase activity to hydrolyze ATP and other kinds of NTPs and dNTPs. For this purpose, we measured the kinetic parameters K_m (the Michaelis constant that describes the amount of substrate needed for the enzyme to obtain half of its maximum rate of reaction) and k_{cat} (a constant that describes the turnover rate of an enzyme-substrate complex to product and enzyme), and indicated the NTPase activity as k_{cat}/K_m (the rate constant that measures catalytic efficiency) of DpTV Hel in the presence of different NTPs and dNTPs. Our results showed that DpTV Hel was able to hydrolyze all NTPs and dNTPs, and the catalytic efficiency of this NTPase with ATP, CTP, GTP, and UTP ranged from 60 to 78 (Table 1). Thus, we conclude that DpTV Hel contains the NTPase activity, which shows no preference to any specific NTP or dNTP.

Optimal reaction conditions for the ATPase activity of DpTV Hel

After determining that DpTV Hel contains the NTPase activity, to further characterize its biochemical properties, we examined

Table 1
Kinetic analysis of NTP and dNTP hydrolysis by DpTV Hel[a].

Substrate	K_m (mM)	k_{cat} (min^{-1})	k_{cat}/K_m ($mM^{-1}\ min^{-1}$)
ATP	0.75 ± 0.06	49.58 ± 3.06	66.04
UTP	0.69 ± 0.03	47.75 ± 1.94	69.63
GTP	1.23 ± 0.14	74.47 ± 7.57	60.65
CTP	0.39 ± 0.02	30.55 ± 1.15	78.18
dATP	2.43 ± 0.31	140.10 ± 17	57.74
dTTP	0.78 ± 0.04	65.99 ± 2.94	84.52
dGTP	1.44 ± 0.13	96.01 ± 8.08	66.92
dCTP	0.74 ± 0.04	40.13 ± 1.77	54.20

[a] Values for K_m and k_{cat} were determined from Lineweaver–Burk plots of hydrolysis activity using the malachite green assay. Reactions were conducted with NTP or dNTP concentrations varying between 0.1 and 1.0 mM, in the presence of 2 mM $MgCl_2$ and 50 mM KCl at pH 7.5. S.D. values were generated from three separate experiments.

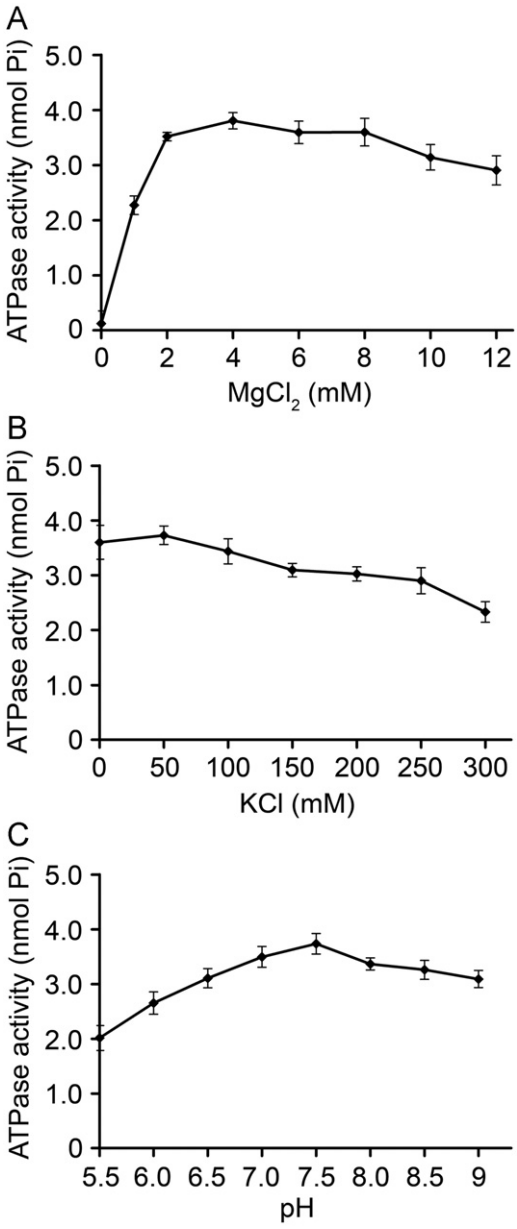

Fig. 5. Optimal conditions for DpTV Hel ATPase activity. (A–C) The ATPase activities were measured as nmol of released inorganic phosphate in 20 μl reaction volume at 37 °C for 20 min, in the presence of indicated concentrations of $MgCl_2$ (A) or KCl (B), or at indicated pH (C). Error bars represent S.D. values from three separate experiments.

its ATPase activity under varying reaction conditions, such as divalent metal ions, salt content and pH. It is noteworthy that ATP is selected as the hydrolysis substrate as it is the major energy source in cells (Hara, 2009). The ATPase activity of DpTV Hel was determined using a sensitive colorimetric assay that measures the total amount of orthophosphate released after each reaction. As shown in Fig. 5A, B and C, 4 mM $MgCl_2$, 50 mM KCl or pH 7.5 was the optimal condition for DpTV Hel to hydrolyze ATP. Comparing with the optimal reaction conditions for DpTV Hel dsRNA unwinding activity (Fig. 4B, D and E), our results show that the optimal conditions for ATPase and unwinding activities of DpTV Hel are similar.

ATPase activities of DpTV Hel and its mutants are stimulated by dsRNA

We have determined that DpTV Hel is an RNA helicase, which also contains an NTPase activity to generate energy for dsRNA unwinding. Thus, it is interesting to examine if the presence of dsRNA or dsDNA has any effect on the NTPase activity of DpTV Hel. For this purpose, DpTV Hel ATPase activity was determined in the absence or presence of standard dsRNA or dsDNA. Our results showed that dsRNA significantly promoted the ATPase activity of DpTV Hel for ~2–2.5 folds compared to that of DpTV Hel alone, while dsDNA showed no effect (Fig. 6A). These results indicate that the oligonucleotide-mediated stimulation of DpTV Hel ATPase activity is also RNA-specific like its duplex unwinding activity.

Previously we have shown that the point mutations of the conversed SF-1 motifs I, II and VI dramatically inhibited the unwinding activity of DpTV Hel (Fig. 2E). Thus, we sought to examine if these mutations can also affect the ATPase activity. To this end, we examined the ATPase activities of DpTV Hel mutants and found that three mutants almost lost all ATPase activity in the absence of dsRNA and dsDNA (Fig. 6B). Interestingly, although dsDNA still showed no effect on the ATPase activity, the presence of dsRNA dramatically stimulated the ATPase activities of these mutants (20–100 fold), resulting in a partial rescue of the mutation-caused loss of ATPase activity to around 40% of wild-type DpTV Hel alone (Fig. 6B).

Taken together, our results demonstrate that dsRNA can not only stimulate DpTV Hel ATPase activity, but also induce a partial rescue of the ATPase activities that were originally abolished by motifs I, II and VI mutations. Consistently, these DpTV Hel mutants exhibited weakened but not abolished dsRNA unwinding activities (Fig. 2E), probably due to the partial recovery of ATPase activities in the presence of dsRNA substrates.

Discussion

Helicases are required for viral replication of many (+)RNA viruses (Ahola et al., 2000; Gu et al., 2000; Lam and Frick, 2006; Mirzayan and Wimmer, 1992; Rikkonen, 1996; van Dinten et al., 2000). Moreover, it may relate to RNA translocation, genome packaging, protection of RNA at the replication center, and modulate RNA–protein interaction (Karpe and Lole, 2010). In this study, we demonstrate that DpTV Hel, the putative helicase domain of DpTV, is a functional RNA helicase with 5′–3′ unwinding directionality. Sequence analysis indicated that DpTV Hel contains all the seven conserved SF-1 motifs, and the mutations in the conserved motifs I, II and VI significantly inhibited DpTV Hel unwinding activity. Based on its conserved SF-1 motifs, specificity for dsRNA, and 5′–3′ unwinding directionality, DpTV Hel belongs to the distinct class of SF1B RNA helicase in the SF-1 superfamily.

Our studies further revealed the length requirement of the 5′ single-stranded tail and the optimal reaction conditions for the dsRNA unwinding activity of DpTV Hel. Moreover, we find that DpTV Hel also contains NTPase activity to hydrolyze ATP as well as other NTPs and dNTPs. The ability of DpTV Hel to hydrolyze ATP could be significantly stimulated by dsRNA but not dsDNA. Interestingly, dsRNA can partially rescue the ATPase activity abolishment caused by motifs I, II and VI mutations.

DpTV Hel showed the 5′–3′ unwinding directionality with the specificity for RNA template strand, and its dsRNA unwinding efficiency is dependent on the length of the 5′ single-stranded tail on the RNA template strand. During viral RNA replication, the 5′ single-stranded tail on RNA template strand can be provided by a replication bubble at the site of nucleotide addition by viral replicase (Warrener and Collett, 1995), and helicase may progress toward dsRNA by a cooperative enzyme binding mechanism to enhance its dsRNA unwinding efficiency (Lee et al., 2010; Wen et al., 2009). Moreover, the dsRNA unwinding and ATPase activities of DpTV Hel are relatively sensitive to reaction environment, including divalent metal ions and K^+ ionic concentrations, and pH (Figs. 4 and 5). These biochemical features indicate that DpTV Hel should function in a limited environment in cells. Indeed, RNA replication of (+)RNA viruses requires viral RNA replicase proteins to associate with intracellular membranes and induce membrane invagination to form small spherules (Ahlquist, 2006; Short and Dorrington, 2012; Short et al., 2010).

To drive dsRNA or dsDNA unwinding, helicases usually hydrolyze NTP, normally ATP, to provide energy (Abdelhaleem, 2010; Manosas et al., 2010). For DpTV, its helicase activity also depends on the presence of ATP (Fig. 2A, lane 5). Moreover, the observation that DpTV Hel can hydrolyze all types of NTPs and dNTPs (Table 1) further confirms its NTPase activity, which can use broad energy sources not limited to ATP. Moreover, we have shown that dsRNA can substantially stimulate DpTV Hel to hydrolyze ATP (Fig. 6A), which is consistent with many other SF-1 helicases whose ATPase activities can be stimulated by oligonucleotides (Gros and Wengler, 1996; Karpe and Lole, 2010; Kim et al., 1999; Seybert et al., 2000; Tanner et al., 2003). It is possible that binding to dsRNA induces a conformational

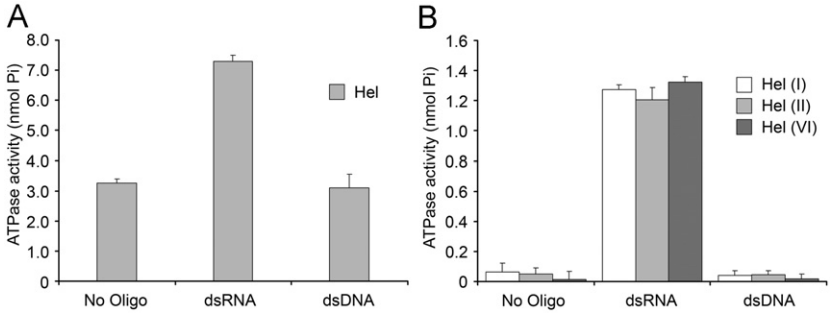

Fig. 6. ATPase activities of DpTV Hel and its mutants are stimulated by dsRNA. The ATPase activity of MBP-Hel (A) or mutants of motifs I, II or VI (B) was determined as in Fig. 5 in the presence of dsRNA or dsDNA. The absence of any oligonucleotide was used as control. Error bars represent S.D. values from three separate experiments.

change on DpTV Hel, which further facilitates DpTV Hel to hydrolyze ATP. However, dsDNA had no effect on the ATPase activity of DpTV Hel (Fig. 6A). Given that dsRNA and dsDNA have different biochemical properties and structures (Kawaoka, 2005), the dsRNA-selective stimulation of DpTV Hel ATPase activity may be due to the protein–dsRNA interaction.

The sequence analysis revealed that DpTV Hel contains all the seven conserved motifs of SF-1 helicase (Fig. 1A). And we found that the abolishment of DpTV Hel ATPase activity was caused by point mutations in motifs I, II and VI, which were reported to be directly involved in ATP hydrolysis and oligonucleotide-binding (Fairman-Williams et al., 2010; Weng et al., 1996). Interestingly, these mutation-induced abolishments of ATPase activity could be partially rescued by dsRNA (Fig. 6B). This recovery of ATPase activity may be caused by the protein–dsRNA interaction that stimulates the abilities of DpTV Hel mutants to hydrolyze ATP. Moreover, DpTV Hel mutants exhibited a weakened but not abolished dsRNA unwinding activities (Fig. 2E), probably due to the partial recovery of ATPase activity in the presence of dsRNA substrates.

To our knowledge, our study is the first to identify a functional helicase from an alphatetravirus, and further provides a detailed characterization of the unwinding and ATPase activities of this nonstructural protein. Our work not only represents an important step toward understanding the mechanism of DpTV dsRNA unwinding, but would also provide directions for future studies of helicases and viral replication of other members of the *Alphatetraviridae* family. Moreover, our identification and characterization of DpTV Hel adds a new member to the SF1B class of the SF1 helicase superfamily.

Materials and methods

Plasmid constructions

Standard procedures were used for extraction of virus genome RNA and reverse transcription-PCR (Zhou et al., 2006; Zhou et al., 2008). A cDNA fragment of the putative DpTV helicase domain (amino acids 523 to 1042 of replicase ORF) was prepared, and mutations were introduced via PCR-mediated mutagenesis as described previously (Yang et al., 2006). The primers used in this study are shown in Table 2. All the fragments were inserted into pFastBac^{TM}HTB-MBP vector, which was originated from the vector pFastBac^{TM}HT-B (Invitrogen, Carlsbad, CA) and modified by our laboratory (Yang et al., 2006), and the resulting plasmid would be used in Bac-to-Bac Baculovirus Expression System to make a fusion protein with an MBP-tag at the N-terminus of DpTV helicase domain.

Protein expression and purification and antibody preparation

The expression and purification of MBP alone and MBP-Hel proteins were carried out as previously described (Yang et al., 2006). Briefly, Sf9 cells at a density of 2×10^6 cells/ml were infected with the recombinant baculoviruses of interest at a MOI of 3 and harvested at 72 h after infection. Cell pellets were resuspended in a binding buffer [20 mM Tris–HCl (pH 7.4), 200 mM NaCl, 1 mM EDTA, 10 mM 2-Mercaptoethanol] supplemented with protease inhibitors cocktail (Sigma, St. Louis, MO, USA). Cells were lysed by sonication and then debris was removed by centrifugation for 30 min at 11,000 g. The protein in the supernatant was purified using amylose affinity chromatography (New England BioLabs, Ipswich, MA), according to the manufacturer's protocol. Collected fractions were analyzed by 12% SDS–PAGE. Fractions containing protein of the expected size were combined and then concentrated using Amicon Ultra-15 filters (Millipore, Schwalbach, Germany), and the buffer was exchanged to 20 mM HEPES-KOH (pH 7.0), 50 mM NaCl and 2 mM dithiothreitol (DTT). Finally, the protein was stored at $-70\ ^{\circ}C$ in aliquots. All proteins were quantified by the Bradford method. The purified MBP-Hel protein was used to immunize rabbits for the production of polyclonal antibodies as previously described (Ye et al., 2012).

Preparation of double-stranded oligonucleotides

Helicase substrates consist of two complementary oligonucleotide strands that were annealed and gel purified. Of the two strands, the larger one was unlabeled and is referred as the template strand. While the smaller strand, referred to as the release strand, was labeled at 5′ end with HEX (Sangon Biotech, Shanghai) (Warrener and Collett, 1995). In this paper, all DNA

Table 2
PCR primers and oligonucleotides used in this study.

Primers[a] or oligonucleotides	Sequence (5′–3′)[b]
Primers	
Hel-F	CGCGGATCCGCCGGCATTTACCGGGTG (BamH I)
Hel-R	CCCAAGCTTCTAAAGGAAGTCAACGTCACGAA (Hind III)
K606E-F	GGCCCACCTGGCAGTGGCGAGACAC
K606E-R	CGAGGAGCTTGCGTGTCTCGCCACT
DE670AA-F	ACTCGTCGTAATCGCCGCATGTTTC
DE670AA-R	GGTAACATGAAACATGCGGCGATTA
TR830AA- F	TTGCTCGTTGGCATTGCCGCTCACA
TR830AA- R	AGATGATTCGTGTGAGCGGCAATGC
oligonucleotides	
RNA1	*CUCCGCUUCAUCCCCAUGC
RNA2	GCAUGGGGAUGAAGCGGAG
RNA3	GGGUUUUGCAUGGGGAUGAAGCGGAGUUUUUUUUUUUUUUUC
RNA4	GGGUUUUUUUUUUUUUGCAUGGGGAUGAAGCGGAGUUUUUUUUUUUUUUUC
RNA5	GGGUUUUUUUGCAUGGGGAUGAAGCGGAGUUUUUUUUUUUUUUC
RNA6	GGGGCAUGGGGAUGAAGCGGAGUUUUUUUUUUUUUUC
RNA7	GCAUGGGGAUGAAGCGGAGUUUUUUUUUUUUUUC
RNA8	GGGUUUUUUUUUUUUUGCAUGGGGAUGAAGCGGAG
DNA1	*CTCCGCTTCATCCCCATGC
DNA2	GGGTTTTTTTTTTTTGCATGGGGATGAAGCGGAGTTTTTTTTTTTTTC

[a] Sequence-specific primers are designed according to GenBank accession numbers AY594352 (DpTV).
[b] Underlined characters indicate restriction endonuclease sites, and the HEX sign at 5′ end of RNA or DNA is shown in asterisk.

strands and HEX-labeled DNA or RNA strands were commercially obtained (Sangon Biotech), and all oligonucleotides in Table 2 were not sequence-specific for viral RNA but designed randomly. Unlabeled RNA strands were synthesized by run-off transcriptions of the PCR products that carry appropriate DNA inserts in the transcription region using T7 RNA polymerase.

To generate oligonucleotide duplexes, the labeled release strand and unlabeled template strand were combined at a molar ratio of approximately 3:1 in 20 mM HEPES-KOH (pH 7.0) and 50 mM KCl. The mixture was heated at 95 °C for 5 min and was then slowly cooled down to room temperature. Annealed products were resolved on 15% native-PAGE, and a band corresponding to double-stranded oligonucleotides was cut from the gel, minced, and soaked in buffer containing 0.5 M ammonium acetate, 10 mM EDTA, and 1% SDS at room temperature for 5 to 6 h for elution. Extracted oligonucleotides were ethanol precipitated and dissolved in nuclease-free water. Standard dsRNA substrate was annealed with RNA1 and RNA3, D*/R substrate was annealed with DNA1 and RNA3, R*/D substrate was annealed with RNA1 and DNA2, D*/D substrate was annealed with DNA1 and DNA2, 5′-tailed substrate was annealed with RNA1 and RNA8, 3′-tailed substrate was annealed with RNA1 and RNA7, and blunt-ended substrate was annealed with RNA1 and RNA2. All DNA and RNA oligonucleotides are listed in Table 2.

Duplex unwinding assays

50 pmol of protein and 0.1 pmol of dsRNA or dsDNA substrate were added to a mixture containing a final concentration of 20 mM HEPES-KOH (pH 7.0), 2.5 mM $MgCl_2$, 2 mM DTT, 50 mM KCl and 5U RNasin (Promega, Madison, WI). The total reaction volume is 10 μl unless otherwise indicated. Reaction was initiated by the addition of 5 mM ATP and incubated at 37 °C for 1 h. To minimize reannealing of the unwound oligonucleotides, a 20-fold molar excess of unlabeled DNA trap, corresponding to release strand, was added at the same time as the reaction terminated. As a positive control, substrates were heat denatured at 95 °C for 5 min in the absence of enzyme. Mixtures were electrophoresed on 10% native-PAGE gels. Gels were scanned with a Typhoon9200 (GE Healthcare, Piscataway, NJ). The ratio of released single strands versus the total of substrates was quantified with ImageQuant software (GE Healthcare).

NTPase assay

NTPase activities were determined using a direct colorimetric assay as previously described (Henkel et al., 1988; Lanzetta et al., 1979). Briefly, a typical NTPase assay was carried out in a 20 μl reaction volume, containing 20 mM HEPES-KOH (pH 7.0), 2.5 mM $MgCl_2$, 2 mM DTT and 10 pmol protein. The NTPase reaction was initiated by the addition of NTP to a final concentration of 1 mM and then incubated at 37 °C for 20 min. When indicated, 25 μg/ml standard dsRNA or dsDNA, which serves as a substrate for DpTV Hel unwinding, was included in the reaction mixture. The reaction was stopped by the addition of EDTA to a final concentration of 20 mM. The color was developed for 5 min following the addition of 80 μl of dye solution (water, 0.0812% malachite green, 5.72% ammonium molybdate in 6 N HCl and 2.32% polyvinyl alcohol were freshly mixed in a 2:2:1:1 ratio, respectively). Then 10 μl of 34% sodium citrate was added and the absorbance at 620 nm was measured after 15 min by using a 96-wellplate reader (Spectra Max M2, USA). The concentration of inorganic phosphate was determined by matching the $A_{620\ nm}$ in a standard curve of $A_{620\ nm}$ versus known standard phosphate concentrations. All the results given with this quantitative assay were the averages of three repeat experiments.

Western blot analyses

Western blot analysis was performed according to our standard procedures (Ye et al., 2012). The polyclonal anti-Hel antibody was described above and used at the dilutions of 1:1000. The anti-MBP antibody was purchased from New England BioLabs, and used at the dilutions of 1:10,000.

Acknowledgments

We thank Mr. Huihui He for his help in protein alignment analysis. This work was supported by the National Natural Science Foundation of China No. 31270189 (to Y. H.), No. 31270190 (to X.Z.) and No. 81201292 (to X.Z.), and the Chinese 111 project (grant B06018).

References

Abdelhaleem, M., 2010. Helicases: an overview. Methods Mol. Biol. 587, 1–12.
Adams, M.J., Carstens, E.B., 2012. Ratification vote on taxonomic proposals to the International Committee on Taxonomy of Viruses (2012). Arch. Virol. 157, 1411–1422.
Ahlquist, P., 2006. Parallels among positive-strand RNA viruses, reverse-transcribing viruses and double-stranded RNA viruses. Nat. Rev. Microbiol. 4, 371–382.
Ahlquist, P., Strauss, E.G., Rice, C.M., Strauss, J.H., Haseloff, J., Zimmern, D., 1985. Sindbis virus proteins nsP1 and nsP2 contain homology to nonstructural proteins from several RNA plant viruses. J. Virol. 53, 536–542.
Ahola, T., den Boon, J.A., Ahlquist, P., 2000. Helicase and capping enzyme active site mutations in brome mosaic virus protein 1a cause defects in template recruitment, negative-strand RNA synthesis, and viral RNA capping. J. Virol. 74, 8803–8811.
Bothner, B., Taylor, D., Jun, B., Lee, K., Siuzdak, G., Schlutz, C., Johnson, J., 2005. Maturation of a tetravirus capsid alters the dynamic properties and creates a metastable complex. Virology 334, 17–27.
Cai, D., Qiu, Y., Qi, N., Yan, R., Lin, M., Nie, D., Zhang, J., Hu, Y., 2010. Characterization of Wuhan Nodavirus subgenomic RNA3 and the RNAi inhibition property of its encoded protein B2. Virus Res. 151, 153–161.
Caruthers, J.M., McKay, D.B., 2002. Helicase structure and mechanism. Curr. Opin. Struct. Biol. 12, 123–133.
Dorrington, R.A., 2011. Tetraviridae. In: Andrew, M.Q., King, Michael J., Adams, Eric B., Carstens, Lefkowitz, E.J (Eds.), Virus Taxonomy. Academic Press, Elsevier, London, UK, pp. 1091–1102.
Fairman-Williams, M.E., Guenther, U.P., Jankowsky, E., 2010. SF1 and SF2 helicases: family matters. Curr. Opin. Struct. Biol. 20, 313–324.
Gorbalenya, A.E., Koonin, E.V., 1993. Helicases: amino acid sequence comparisons and structure–function relationships. Curr. Opin. Struct. Biol. 3, 419–429.
Gorbalenya, A.E., Koonin, E.V., Donchenko, A.P., Blinov, V.M., 1988. A conserved NTP-motif in putative helicases. Nature 333, 22.
Gorbalenya, A.E., Koonin, E.V., Donchenko, A.P., Blinov, V.M., 1989. Two related superfamilies of putative helicases involved in replication, recombination, repair and expression of DNA and RNA genomes. Nucl. Acids Res. 17, 4713–4730.
Gordon, K.H., Johnson, K.N., Hanzlik, T.N., 1995. The larger genomic RNA of *Helicoverpa armigera* stunt tetravirus encodes the viral RNA polymerase and has a novel 3′-terminal tRNA-like structure. Virology 208, 84–98.
Gordon, K.H., Williams, M.R., Hendry, D.A., Hanzlik, T.N., 1999. Sequence of the genomic RNA of nudaurelia beta virus (*Tetraviridae*) defines a novel virus genome organization. Virology 258, 42–53.
Gros, C., Wengler, G., 1996. Identification of an RNA-stimulated NTPase in the predicted helicase sequence of the Rubella virus nonstructural polyprotein. Virology 217, 367–372.
Gu, B., Liu, C., Lin-Goerke, J., Maley, D.R., Gutshall, L.L., Feltenberger, C.A., Del Vecchio, A.M., 2000. The RNA helicase and nucleotide triphosphatase activities of the bovine viral diarrhea virus NS3 protein are essential for viral replication. J. Virol. 74, 1794–1800.
Hanzlik, T.N., Gordon, K.H., 1997. The *Tetraviridae*. Adv. Virus Res. 48, 101–168.
Hara, K.Y., 2009. Permeable cell assay: a method for high-throughput measurement of cellular ATP synthetic activity. Reverse Chem. Genet. 577, 251–258.
Henkel, R.D., VandeBerg, J.L., Walsh, R.A., 1988. A microassay for ATPase. Anal Biochem. 169, 312–318.
Hodgman, T.C., 1988. A new superfamily of replicative proteins. Nature 333, 22–23.
Huang, Y., Liu, Z.R., 2002. The ATPase, RNA unwinding, and RNA binding activities of recombinant p68 RNA helicase. J. Biol. Chem. 277, 12810–12815.
Johnson, J.E., Munshi, S., Liljas, L., Agrawal, D., Olson, N.H., Reddy, V., Fisher, A., McKinney, B., Schmidt, T., Baker, T.S., 1994. Comparative studies of $T=3$ and $T=4$ icosahedral RNA insect viruses. Arch. Virol. Suppl. 9, 497–512.

Karpe, Y.A., Lole, K.S., 2010. NTPase and 5′ to 3′ RNA duplex-unwinding activities of the hepatitis E virus helicase domain. J. Virol. 84, 3595–3602.
Kawaoka, J., 2005. Choosing between DNA and RNA: the polymer specificity of RNA helicase NPH-II. Nucleic Acids Res. 33, 644–649.
Kim, H.D., Choe, J., Seo, Y.S., 1999. The sen1(+) gene of *Schizosaccharomyces pombe*, a homologue of budding yeast SEN1, encodes an RNA and DNA helicase. Biochemistry 38, 14697–14710.
Koonin, E.V., Gorbalenya, A.E., Purdy, M.A., Rozanov, M.N., Reyes, G.R., Bradley, D.W., 1992. Computer-assisted assignment of functional domains in the nonstructural polyprotein of hepatitis E virus: delineation of an additional group of positive-strand RNA plant and animal viruses. Proc. Natl Acad. Sci. 89, 8259–8263.
Lam, A.M., Frick, D.N., 2006. Hepatitis C virus subgenomic replicon requires an active NS3 RNA helicase. J Virol. 80, 404–411.
Lanzetta, P.A., Alvarez, L.J., Reinach, P.S., Candia, O.A., 1979. An improved assay for nanomole amounts of inorganic phosphate. Anal Biochem. 100, 95–97.
Lee, N.R., Kwon, H.M., Park, K., Oh, S., Jeong, Y.J., Kim, D.E., 2010. Cooperative translocation enhances the unwinding of duplex DNA by SARS coronavirus helicase nsP13. Nucleic Acids Res. 38, 7626–7636.
Lohman, T.M., Bjornson, K.P., 1996. Mechanisms of helicase-catalyzed DNA unwinding. Annu. Rev. Biochem. 65, 169–214.
Mackintosh, S.G., Raney, K.D., 2006. DNA unwinding and protein displacement by superfamily 1 and superfamily 2 helicases. Nucleic Acids Res. 34, 4154–4159.
Manosas, M., Xi, X.G., Bensimon, D., Croquette, V., 2010. Active and passive mechanisms of helicases. Nucleic Acids Res. 38, 5518–5526.
Mirzayan, C., Wimmer, E., 1992. Genetic analysis of an NTP-binding motif in poliovirus polypeptide 2C. Virology 189, 547–555.
Odegard, A., Banerjee, M., Johnson, J.E., 2010. Flock house virus: a model system for understanding non-enveloped virus entry and membrane penetration. Curr. Top Microbiol. Immunol. 343, 1–22.
Olson, N.H., Baker, T.S., Johnson, J.E., Hendry, D.A., 1990. The three-dimensional structure of frozen-hydrated *Nudaurelia capensis* beta virus, a $T=4$ insect virus. J. Struct. Biol. 105, 111–122.
Pringle, F.M., Gordon, K.H., Hanzlik, T.N., Kalmakoff, J., Scotti, P.D., Ward, V.K., 1999. A novel capsid expression strategy for *Thosea asigna* virus (*Tetraviridae*). J. Gen. Virol. 80, 1855–1863.
Pyle, A.M., 2008. Translocation and unwinding mechanisms of RNA and DNA helicases. Annu. Rev. Biophys. 37, 317–336.
Qi, N., Cai, D., Qiu, Y., Xie, J., Wang, Z., Si, J., Zhang, J., Zhou, X., Hu, Y., 2011. RNA binding by a novel helical fold of B2 protein from Wuhan Nodavirus Mediates the Suppression of RNA interference and promotes B2 dimerization. J. Virol. 85, 9543–9554.
Qi, N., Zhang, L., Qiu, Y., Wang, Z., Si, J., Liu, Y., Xiang, X., Xie, J., Qin, C.F., Zhou, X., Hu, Y., 2012. Targeting of Dicer-2 and RNA by a viral RNA silencing suppressor in *Drosophila* cells. J. Virol. 86, 5763–5773.
Qiu, Y., Cai, D., Qi, N., Wang, Z., Zhou, X., Zhang, J., Hu, Y., 2011. Internal initiation is responsible for synthesis of *Wuhan nodavirus* subgenomic RNA. J. Virol. 85, 4440–4451.
Rikkonen, M., 1996. Functional significance of the nuclear-targeting and NTP-binding motifs of Semliki Forest virus nonstructural protein nsP2. Virology 218, 352–361.
Sabanadzovic, S., Ghanem-Sabanadzovic, N.A., Gorbalenya, A.E., 2009. Permutation of the active site of putative RNA-dependent RNA polymerase in a newly identified species of plant alpha-like virus. Virology 394, 1–7.
Seybert, A., Hegyi, A., Siddell, S.G., Ziebuhr, J., 2000. The human coronavirus 229E superfamily 1 helicase has RNA and DNA duplex-unwinding activities with 5′-to-3′ polarity. RNA (New York, N.Y.) 6, 1056–1068.
Shen, J.C., Gray, M.D., Oshima, J., Loeb, L.A., 1998. Characterization of Werner syndrome protein DNA helicase activity: directionality, substrate dependence and stimulation by replication protein A. Nucleic Acids Res. 26, 2879–2885.
Short, J.R., Dorrington, R.A., 2012. Membrane targeting of an alpha-like tetravirus replicase is directed by a region within the RNA-dependant RNA polymerase domain. J. Gen. Virol.
Short, J.R., Knox, C., Dorrington, R.A., 2010. Subcellular localization and live-cell imaging of the *Helicoverpa armigera* stunt virus replicase in mammalian and *Spodoptera frugiperda* cells. J. Gen. Virol. 91, 1514–1523.
Singleton, M.R., Dillingham, M.S., Wigley, D.B., 2007. Structure and mechanism of helicases and nucleic acid translocases. Annu. Rev. Biochem. 76, 23–50.
Speir, J.A., Johnson, J.E., 2008. Tetraviruses. In: Mahy., B.W.J., Regenmortel., M.H.V.V. (Eds.), Desk Encyclopedia of General Virology. Academic Press, San Diego, CA, pp. 27–37.
Speir, J.A., Taylor, D.J., Natarajan, P., Pringle, F.M., Ball, L.A., Johnson, J.E., 2010. Evolution in action: N and C termini of subunits in related $T=4$ viruses exchange roles as molecular switches. Structure 18, 700–709.
Tang, J., Lee, K.K., Bothner, B., Baker, T.S., Yeager, M., Johnson, J.E., 2009. Dynamics and stability in maturation of a $T=4$ virus. J. Mol. Biol. 392, 803–812.
Tanner, J.A., Watt, R.M., Chai, Y.B., Lu, L.Y., Lin, M.C., Peiris, J.S., Poon, L.L., Kung, H.F., Huang, J.D., 2003. The severe acute respiratory syndrome (SARS) coronavirus NTPase/helicase belongs to a distinct class of 5′ to 3′ viral helicases. J. Biol. Chem. 278, 39578–39582.
Taylor, D.J., Krishna, N.K., Canady, M.A., Schneemann, A., Johnson, J.E., 2002. Large-scale, pH-dependent, quaternary structure changes in an RNA virus capsid are reversible in the absence of subunit autoproteolysis. J. Virol. 76, 9972–9980.
Taylor, D.J., Speir, J.A., Reddy, V., Cingolani, G., Pringle, F.M., Ball, L.A., Johnson, J.E., 2006. Preliminary x-ray characterization of authentic providence virus and attempts to express its coat protein gene in recombinant baculovirus. Arch. Virol. 151, 155–165.
Teterina, N.L., Kean, K.M., Gorbalenya, A.E., Agol, V.I., Girard, M., 1992. Analysis of the functional significance of amino acid residues in the putative NTP-binding pattern of the poliovirus 2C protein. J. Gen. Virol. 73, 1977–1986.
Tomasicchio, M., Venter, P.A., Gordon, K.H., Hanzlik, T.N., Dorrington, R.A., 2007. Induction of apoptosis in *Saccharomyces cerevisiae* results in the spontaneous maturation of tetravirus procapsids in vivo. J. Gen. Virol. 88, 1576–1582.
van Dinten, L.C., van Tol, H., Gorbalenya, A.E., Snijder, E.J., 2000. The predicted metal-binding region of the arterivirus helicase protein is involved in subgenomic mRNA synthesis, genome replication, and virion biogenesis. J. Virol. 74, 5213–5223.
Walter, C.T., Pringle, F.M., Nakayinga, R., de Felipe, P., Ryan, M.D., Ball, L.A., Dorrington, R.A., 2010. Genome organization and translation products of Providence virus: insight into a unique tetravirus. J. Gen. Virol. 91, 2826–2835.
Walukiewicz, H.E., Johnson, J.E., Schneemann, A., 2006. Morphological changes in the $T=3$ capsid of Flock House virus during cell entry. J. Virol. 80, 615–622.
Wang, X., Lee, W.M., Watanabe, T., Schwartz, M., Janda, M., Ahlquist, P., 2005. Brome mosaic virus 1a nucleoside triphosphatase/helicase domain plays crucial roles in recruiting RNA replication templates. J. Virol. 79, 13747–13758.
Warrener, P., Collett, M.S., 1995. Pestivirus NS3 (p80) protein possesses RNA helicase activity. J. Virol. 69, 1720–1726.
Wen, G., Xue, J., Shen, Y., Zhang, C., Pan, Z., 2009. Characterization of classical swine fever virus (CSFV) nonstructural protein 3 (NS3) helicase activity and its modulation by CSFV RNA-dependent RNA polymerase. Virus Res. 141, 63–70.
Weng, Y., Czaplinski, K., Peltz, S.W., 1996. Genetic and biochemical characterization of mutations in the ATPase and helicase regions of the Upf1 protein. Mol. Cell. Biol. 16, 5477–5490.
Yang, B., Zhang, J., Cai, D., Li, D., Chen, W., Jiang, H., Hu, Y., 2006. Biochemical characterization of *Periplaneta fuliginosa* densovirus non-structural protein NS1. Biochem. Biophys. Res. Commun. 342, 1188–1196.
Ye, S., Xia, H., Dong, C., Cheng, Z., Xia, X., Zhang, J., Zhou, X., Hu, Y., 2012. Identification and characterization of Iflavirus 3C-like protease processing activities. Virology.
Yi, F., Zhang, J., Yu, H., Liu, C., Wang, J., Hu, Y., 2005. Isolation and identification of a new tetravirus from *Dendrolimus punctatus* larvae collected from Yunnan Province, China. J. Gen. Virol. 86, 789–796.
Zeddam, J.L., Gordon, K.H., Lauber, C., Alves, C.A., Luke, B.T., Hanzlik, T.N., Ward, V.K., Gorbalenya, A.E., 2010. Euprosterna elaeasa virus genome sequence and evolution of the *Tetraviridae* family: emergence of bipartite genomes and conservation of the VPg signal with the dsRNA Birnaviridae family. Virology 397, 145–154.
Zhou, L., Zhang, J., Wang, X., Jiang, H., Yi, F., Hu, Y., 2006. Expression and characterization of RNA-dependent RNA polymerase of *Dendrolimus punctatus* tetravirus. J. Biochem. Mol. Biol. 39, 571–577.
Zhou, L., Zheng, Y., Jiang, H., Zhou, W., Lin, M., Han, Y., Cao, X., Zhang, J., Hu, Y., 2008. RNA-binding properties of *Dendrolimus punctatus* tetravirus p17 protein. Virus Res. 138, 1–6.